Least mean square based adaptive control of active power filter

Ramavath Chander[1], Edara Venkata Chandra Sekhara Rao[2], Erukula Vidyasagar[1]
[1]Department of Electrical Engineering, University College of Engineering (A), Osmania University, Hyderabad, India
[2]Department of Electrical and Electronics Engineering, Associate Professor, MVSR Engineering College, Hyderabad, India

Article Info

ABSTRACT

The proposed control scheme is based on the least mean square (LMS) algorithm. The LMS algorithm is employed to estimate the necessary reference tracking current for the active power filter (APF). The proposed control scheme aims to enhance the dynamic response of the APF and minimize steady-state error. The weights of the LMS technique are calculated based on the estimated current of the APF. This algorithm is employed to minimize the error difference between the desired system output and its actual output, known as the mean square error (MSE). The estimated weights are utilized to modify the reference current weights, enabling them to follow the intended current of the APF. The online adaption of the LMS method involves the real-time adjustment of the weights. The performance of the LMS-based APF control is evaluated through a simulation study in MATLAB/Simulink, where it is compared with the conventional control method.

Corresponding Author:

Ramavath Chander
Department of Electrical Engineering, University College of Engineering (A), Osmania University
Hyderabad, Telangana, India
Email: chanderou19@gmail.com

NOMENCLATURE

$i_{mL}(t)$: Nonlinear load current 16	$i_{mq}(t)$ reactive current	$p_{mp}(t)$: Active load power
i_{m1} : Maximum nonlinear current 17		$p_{mq}(t)$: Reactive load power
$i_{mh}(t)$: Harmonics component current		$p_{mh}(t)$: Harmonics load power
Φ_1 : Angle between voltage and current 18		I_{sp} : The peak amplitude of the desired source current
V_{dc} : Capacitor dc link voltage		I_{sl} : Loss current
$V_s(t)$; Source voltage 19 W weight		$I_c(t)$: Compensation current
V_m : Maximum voltage 20 η learning rate		$I_s(t)$: Source current
$p_L(t)$: Load power 21 V_{dcref} Reference voltage		$i_{mp}(t)$: Active current
i_L : Load current		

1. INTRODUCTION

The diode bridge rectifier is a simple and cost-effective solution for converting alternating current (AC) power to direct current (DC) power. It is commonly used in applications such as power supplies, battery chargers, and motor drives. The thyristor-controlled rectifier is a more advanced power converter that provides higher efficiency. However, these types of converters are the source of harmonics and cause the low power factor and harmonics distortion in the supply current. The harmonics current causes the mal operation of sophisticated system such as torque ripple in the adjustable speed control drives, electromagnetic

interferences (EMI) and electromagnetic compatibility (EMC) in electronics components [1]. The power developed by the harmonics current not useful and needs to be suppressed. Conventionally, passive filters which are realized with the different combination of inductor and capacitor and are used to eliminates the harmonics and reactive current caused by the nonlinear load. However, the passive filters have the drawbacks of series or parallel resonance, the performance characteristics are influenced by the source impedance, fixed compensation current and aging issues. In order to alleviate the problems caused by the passive filter, an active power filter based on the power semi-conductor devices and micro-electronics are realized in the literature [1]. The active power filter offers the various functions such as harmonics current mitigations, reactive power compensation, neutral line current suppression, voltage regulation and load termination etc. the multiple dynamics compensation characteristics offered by the active power at low cost and smaller volt-ampere rating [2]–[5]. However, the performance characteristics active power filter is not influenced by the load and provides reliable operations.

The active power filter (APF) compensation performance mostly influenced by the control method which is employed to track desired reference current [6]. The control scheme is used for the APF have two loops and outer loop is used to regulate the DC link voltage and provides the path for exchange of oscillating power between source and APF. Another inner loop is employed to regulate the current of APF. Uncontrolled current in the inner loop leads to saturation of controller limits and increase the APF current. The excess current leads to damage the semi-conductors switches in the APF. Many controllers have been reported in the literature to regulate the DC link voltage of APF such as proportional integral (PI) controller, fuzzy logic controller, adaptive neuro-fuzzy inference system-based controller, sliding mode controllers [7]–[9]. However, most of these controllers have been used to improve the steady state and dynamic performance of the APF.

Many control schemes have been reported in the literature to estimate the reference current to track desired sinusoidal current with APF. The most widely employed reference current estimating methods are synchronous reference frame (SRF) and instantaneous reactive power theory [10]-[21]. In SRF all three phase quantities are transformed into the d-q-quantities using park transformation and consequent computation of reference current for the APF [22]–[25]. In instantaneous reactive power theory, all quantities such as voltage and load currents are transformed into two-phase and computation power and consequent computation of reference current to track desired current with APF. However, both synchronous reference frame and instantaneous theory requires transformation of quantities into two-phase and subsequent inverse transformations for computation of the reference current for the APF.

In this paper, control based on conventional control theory and least mean square based conventional control theory is used for the estimation of the reference current for the APF. The LMS based conventional control theory not requires number complex transformation and it requires simple addition, subtraction for the computation of reference current of the APF.

2.   TOPOLOGY OF APF

The APF system is illustrated in Figure 1. The APF system comprises a supply system, a load, and an active power filter realized using power semi-conductor. The voltage source inverter is implemented using an inductor, capacitor and insulated gate bipolar transistor (IGBT).
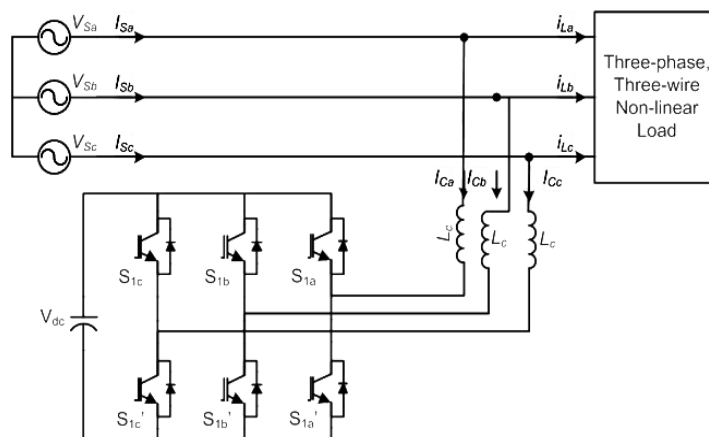

Figure 1. Topology of the APF

The non-linear load system is realized using a diode bridge rectifier. The non-linear load is created by employing a diode bridge rectifier with commutation inductor and a capacitor on the DC side. The APF is connected to the point of common coupling using an inductor to effectively eliminate the switching noise generated by the switching components. The DC link capacitor is situated on the DC side of the voltage source inverter, serving the purpose of reducing the voltage fluctuations resulting from the operation of the semi-conductor devices. The APF employing to introduce the corrective harmonic currents at the point of common coupling using an inductor, with the intention of neutralizing the harmonics introduced by non-linear loads. The APF play a crucial role in maintaining a clean and stable power supply by mitigating harmonics, reactive power, and other power quality issues introduced by non-linear loads.

3.   CONTROL METHOD OF APF

The control strategy of the active power filter is utilized to derive the reference current. The reference currents are employed to follow the intended source current using the APF. The reference currents are used to track the desired source current with the APF.

3.1. Conventional control method of APF

The current caused by the non-linear load is denoted by the subsequent in (1);

$$i_{mL}(t) = i_{m1} \cos(\phi_1) \sin(\omega t) + i_{m1} \sin(\phi_1) \cos(\omega t) + \sum_{n=2}^{\infty} i_{mn} \sin(n\omega t + \phi_n) \tag{1}$$

The supply voltage is given as in (2).

$$v_s(t) = V_m \sin(\omega t) \tag{2}$$

The instantaneous load power can be expressed in (3).

$$p_L(t) = v_s(t) \times i_L(t)$$
$$i_{mL}(t) = V_m i_{m1} \cos(\phi) \sin^2(\omega t) + V_m \sin(\omega t) i_{m1} \sin(\phi) \cos(\omega t)$$
$$+ V_m \sin(\omega t) \sum_{n=2}^{\infty} i_{mn} \sin(n\omega t + \phi_n) \tag{3}$$

The load power can be expressed in (4).

$$p_L(t) = p_{mp}(t) + p_{mq}(t) + p_{mh}(t) \tag{4}$$

From (4), active power demand of the load is expressed as (5).

$$p_{mp}(t) = V_m I_{m1} \sin^2(\omega t) \times \cos(\phi_1) = v_s(t) \times i_{mp}(t) \tag{5}$$

From (5), after harmonics current mitigation with active power filter and supply current is expressed as (6);

$$i_{mp}(t) = \frac{p_{mp}(t)}{v_s(t)} = I_1 \sin(\omega t) \times \cos(\phi_1) = I_{sm} \sin(\omega t) \tag{6}$$

where $I_{sm} = I_{m1} \cos(\phi_1)$. In actual practice, the DC link capacitor and APF switches are causes the switching losses. Consequently, the supply needs to provide both the active power and the power losses of the APF. The maximum value of the supply current is represented by (7).

$$I_{sp} = I_{sm} + I_{sl} \tag{7}$$

Where I_{sl} is used to represent the peak value of loss current. After the reduction of harmonics current through APF, the resultant current tends to become sinusoidal in nature and synchronizes with the voltage of the power source. The APF current is represented by (8).

$$i_c(t) = i_L(t) - i_s(t) \tag{8}$$

The desired source current, subsequent to harmonics suppression using the APF as shown in (9).

$$i_{sa}^* = I_{sp}\,sin(\omega t)$$
$$i_{sb}^* = I_{sp}\,sin\left(\omega t - \frac{2\pi}{3}\right)$$
$$i_{sb}^* = I_{sp}\,sin\left(\omega t - \frac{4\pi}{3}\right) \tag{9}$$

Where I_{sp} is used to represent the peak amplitude of the desired source current after harmonics compensation with APF. The peak amplitude of the source current is multiplied with unit templates computed using source voltages. The product of the peak amplitude current and unit template is used represent the desired source current. The desired current is compared with measured current and sent to the hysteresis controller. The hysteresis controller is employed to generate the switching pulses the power semi-conductor devices.

3.2. Least mean square-based control method for APF

The load current is expressed as (10).

$$i_{mL}(t) = i_{m1}\,cos(\phi_1)\,sin(\omega t) + i_{m1}\,sin(\phi_1)\,cos(\omega t)$$
$$+ \sum_{n=2}^{\infty} i_{mn}\,sin(n\omega t + \phi_n)$$
$$= i_{mp}(t) + i_{mq}(t) + i_{mh}(t) \tag{10}$$

The active component of the current can be expressed as (11).

$$i_{mp}(t) = \frac{p_{mp}(t)}{v_s(t)} = I_1\,sin(\omega t) \times cos(\phi_1)$$
$$i_{mp}(t) = W\,sin(\omega t) \tag{11}$$

where $i_{mp}(t)$ is used to represents the active component of the current and $W = i_1\,cos(\phi_1)$ is the weight. The weight is estimated from the change in the load current. The load current can be written as (12).

$$i_{mL} = i_{mp}(t) + i_c(t) \tag{12}$$

After harmonics mitigation with active power filter, the current of APF is expressed as (13).

$$i_c(t) = i_{mq}(t) + i_{mh}(t) \tag{13}$$

The APF inject the reactive and harmonics current so that the supply current tends to sinusoidal waveform. At this instant supply current is the in-phase supply voltage. The compensating current supplied by the active power filter in (14).

$$i_c(t) = i_{mL}(t) - i_{mp}(t) \tag{14}$$

According to (11) is substituted in (14) and the value of the current supplied by the APF in (15).

$$i_c(t) = i_{mL}(t) - W\,sin(\omega t) \tag{15}$$

The weight W is calculated based on the changes caused of the load current and supply voltage of the utility. The weight is calculated using least mean square method based on adaptive neural network approach. The neural network based on LMS method is depicted in Figure 2.

The adaptive neural network consist of adaptive linear element and weight is W and bias is made to zero. The input to adaptive neural network is the supply voltage $V_s(t)$ and output of the neural network is the active current $i_{mp}(t)$ and output of the adaptive neural network is the reference current $i_{mf}(t)$ to the APF. As per the least mean square method based on Widrow-Hoff rule, the iterative weight updated equation is expressed as (16).

$$W_{(n+1)} = W_{(n)} + \eta i_c\,sin(\omega t) \tag{16}$$

Where $\eta i_c\,sin(\omega t)$ is used to represents the change in weight with nonlinear load current and supply voltage. From equations, the proposed control scheme based on the adaptive neural network is shown in Figure 3. The weight (W) of neural network is updated with Widrow-off learning rule. Then the reference current is computed with (16) is used for the APF to track desired reference current. After computation of reference current with adaptive neural network, the reference current is presented to obtain the signals for the switches

of voltage source inverter based APF. Figure 3 control schemes 3. Figure 3(a) shown the LMS algorithm, Figure 3(b) shown the control scheme of the APF.
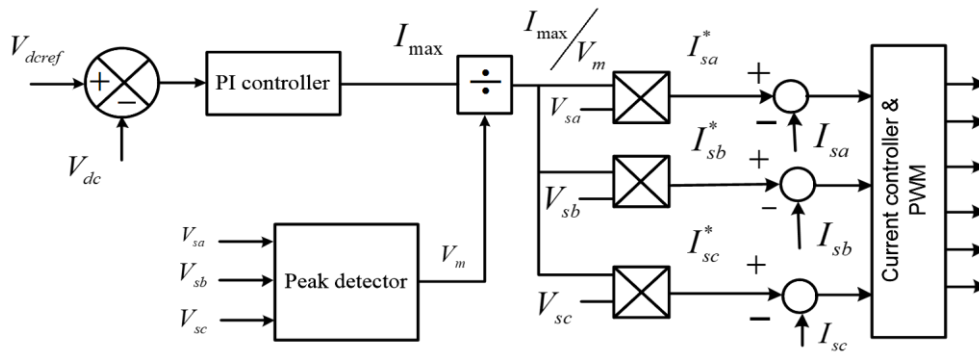

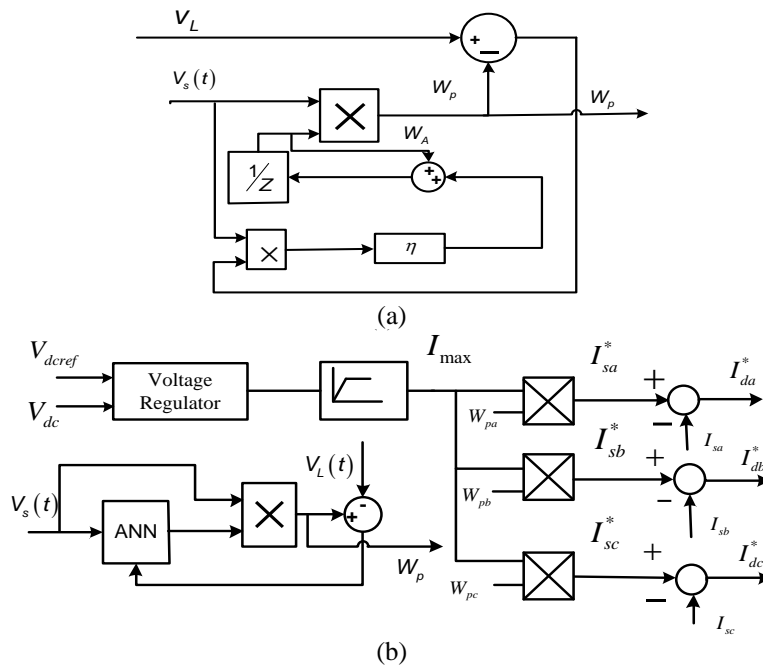Figure 2. Control scheme based on conventional control [26]

(a)

(b)

Figure 3. Control schemes (a) LMS algorithm and (b) control scheme of the APF

4. SIMULATION RESULTS AND ANALYSIS

The computer-based simulation of the APF is carried out using MATLAB/Simulink with Sim power systems block sets. The APF is developed using the power electronics library, while corresponding control strategy is constructed using widely used block sets and control system libraries. Additionally, the non-linear load is created using Sim power system block sets and power electronics diode bridge module. The estimation of the reference tracking current for the APF is accomplished by considering the load current, source current, and supply voltage of the electrical power system. The estimated source current is directed to the hysteresis controller to produce the switching signals that drive the insulated gate bipolar transistor of the presented APF. The adaptive neural network's weight is iteratively updated using the LMS algorithm for the reference current. The simulated results achieved using APF is illustrated in Figure 4. The various waveforms depicting the characteristics of the APF include utility voltage, utility current, load current, and APF current respectively. Before, compensation with APF, the source current is identical to the load current and the source voltage and currents are not synchronized in phase. The source current is highly distorted and exhibits

a waveform characteristic as stepped-shape waveforms. It can be observed from Figure 4(a). At t=0.3 sec., the load current is changed from 24 A to the 38 A resulting in changes to the source current and APF current to meet the load demand caused by load current change. And observed from Figure 4(b). The total harmonics distortion (THD) before the harmonics current mitigation can be observed in Figure 4(c) and its value is 15.06%. At t=0.1 seconds, after mitigating harmonics with APF, the source current waveforms changed from a non-sinusoidal waveform with a stepped shape to sinusoidal waveform. The APF current compensates for the variations in load currents. The source current reaches a steady state within three cycles. After being compensated by the APF it is observed in Figure 4(d), the total harmonics distortion is lowered to 4.54%.

(a)

(b)
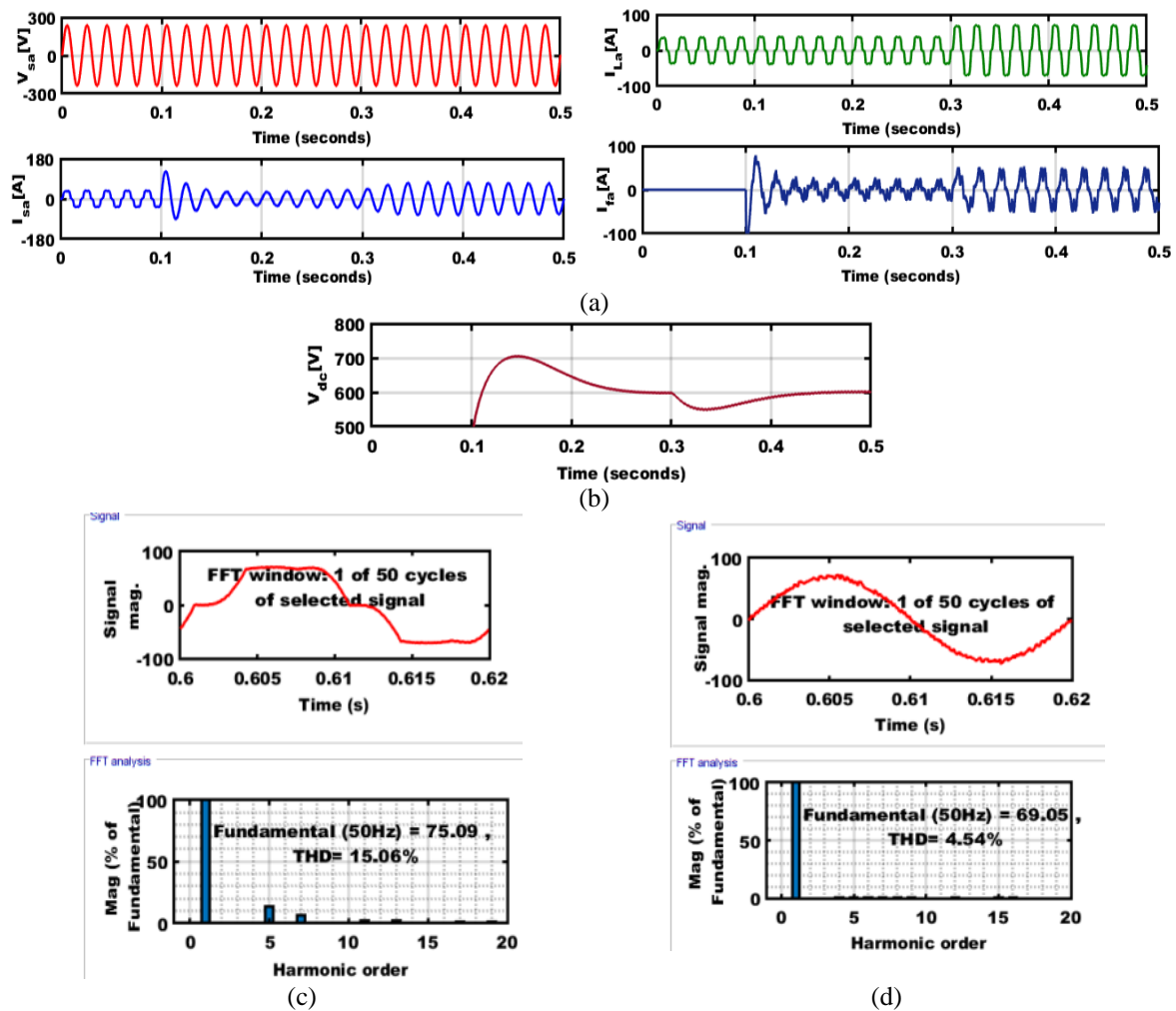

(c)   (d)

Figure 4. Performance of the APF with conventional control method (a) Source voltage, source current, load current, APF current, (b) DC link voltage, (c) % of THD without compensation, and (d) % of THD with compensation

Performance of APF with LMS based control schemes shown in Figure 5. The waveform is shown in Figure 5(a). The waveform of the APF DC link voltage is shown in Figure 5(b). At t=-0.1sec., the DC link voltage reaches a steady state around 0.1 sec. The DC link voltage waveform exhibits a gradual increase and reaches a steady state in approximately 50 ms. At t=0.3 sec., the rapid decrease in the DC link voltage is a result of the step-change in load current. The drop in DC link voltage is utilized to fulfill the load current requirement, ensuring that the source current remains unaffected by the load demand. The waveform of the DC link voltage in response to load variations is shown in Figure 4(b).

The simulated results obtained using the APF with LMS based control method are shown in Figures 5(a)-5(d). As evident from the waveforms before harmonics current mitigation with APF, the source current waveforms contain harmonics and exhibit non-sinusoidal characteristics. The harmonics distortion factor can be seen from Figure 5(c). After harmonics current mitigation performed by the APF, the

source current waveform transforms into a sinusoidal shape and becomes aligned in phase with the supply utility voltage. At t=0.3 Sec., the load current is suddenly increased which results in rise in source current to mitigate the load demand. The settling time of source current to attain the steady state is almost 2 cycles. The load current causes the sudden drop in the DC link voltage of APF which is used to mitigate the load demand. The DC link voltage of APF is gradually restored to its reference value within 0.1s. As it can be seen from the simulated characteristics of the APF, the LMS based control method exhibit the better characteristics than that of the conventional method of APF. The comparative performance characteristic of APF with different controller scheme is shown in Table 1. From the Table 1, it can be observed that the steady state performance of the APF with different control scheme such as IRPT control scheme, SRF control scheme, conventional control scheme based on the PI controller and LMS based controller is identical. As it can be seen from the Table 2, the transient performance of the LMS based control scheme better than the other control schemes. The presence of low pass filter delays the response in the IRPT method and synchronous reference frame control method of APF.
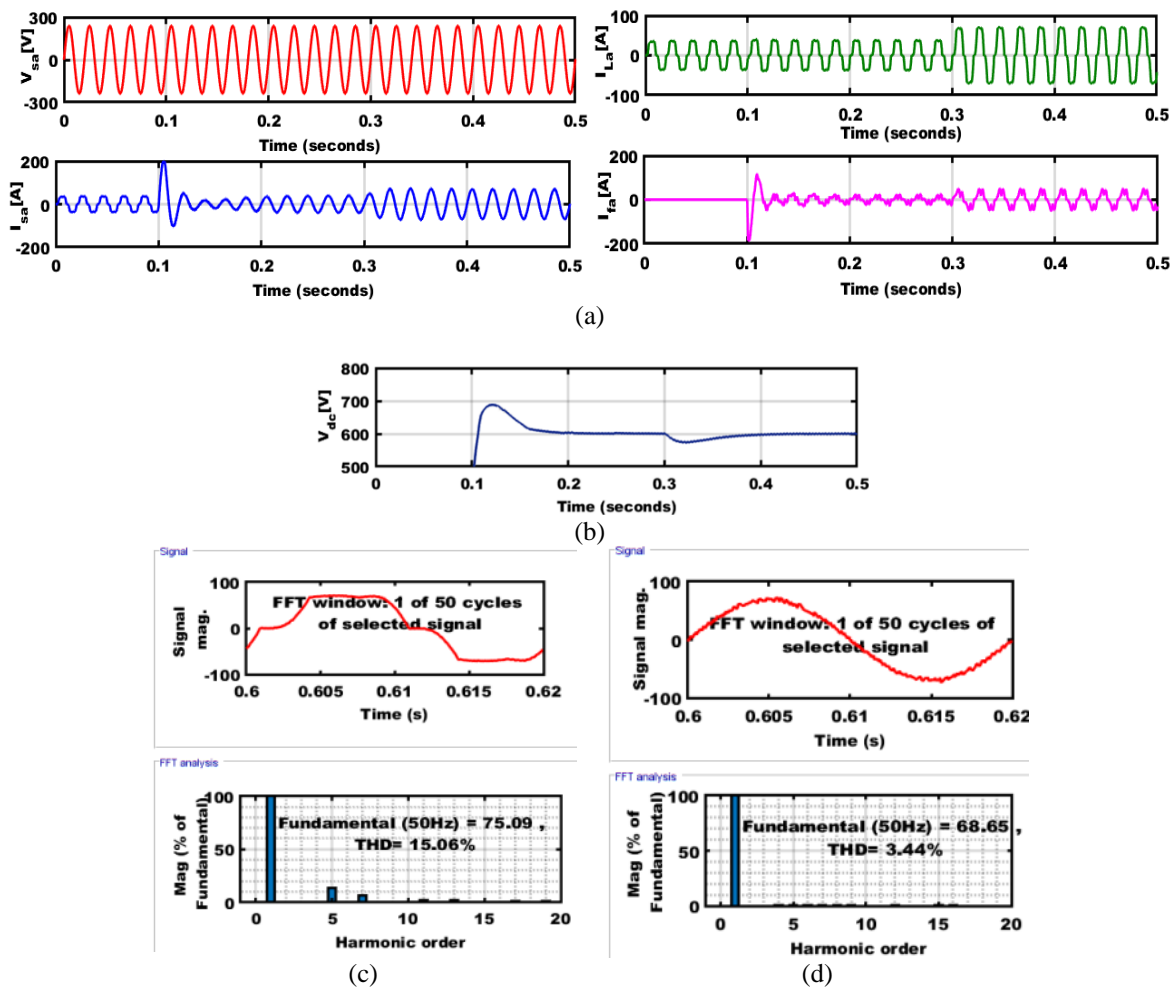

Figure 5. Performance of APF with LMS based control schemes (a) source voltage, source current, load current, APF current, (b) DC link voltage, (c) % of THD without compensation, and (d) % of THD with compensation

Table 1. Comparison of conventional control and LMS based control scheme

Load current in phases	Load current THD	Source current THD with conventional control scheme	Source current THD with IRPT control method [15]	Source current THD with SRF control method [2]	Source current THD with LMS-control scheme
Phase-a	15.06%	3.49%	3.45%	3.45%	3.44%
Phase-b	15.06%	3.45%	3.45%	3.45%	3.45%
Phase-c	15.06%	3.45%	3.44%	3.44%	3.44%

Table 2. Comparison of conventional control and LMS based scheme

	Conventional control method [26]	IRPT control method [15]	SRF control method [2]	LMS based control method
Settling time	0.24 s	0.1 s	0.11 s	0.1 s

5. CONCLUSION

The APF control scheme originated from the conventional control theory and is employed to reduce the harmonics generated by nonlinear load. The conventional control strategy's performance characteristics are enhanced when integrated with LMS algorithm-based control strategy. This combination results in improved effectiveness and performance of the overall system. The LMS algorithm is used for estimate the reference from the voltage and load current as input. The simulation results show that the LMS-based conventional control scheme performs better than the conventional control scheme. Thus, the conventional control- scheme can be substituted with an enhanced conventional control scheme that utilizes the LMS algorithm without introducing any distortion in the characteristics of the APF.

REFERENCES

[1] S. Buso, L. Malesani, and P. Mattavelli, "Comparison of current control techniques for active filter applications," *IEEE Transactions on Industrial Electronics*, vol. 45, no. 5, pp. 722–729, 1998, doi: 10.1109/41.720328.
[2] D. M. Divan, S. Bhattacharya, and B. Banerjee, "Synchronous frame harmonic isolator using active series filter," in *European conference on power electronics and applications*, 1992, pp. 3030–3035.
[3] P. Verdelho and G. D. Marques, "Four-wire current-regulated PWM voltage converter," *IEEE Transactions on Industrial Electronics*, vol. 45, no. 5, pp. 761–770, 1998, doi: 10.1109/41.720333.
[4] A. Chandra, B. Singh, B. N. Singh, and K. Al-Haddad, "An improved control algorithm of shunt active filter for voltage regulation, harmonic elimination, power-factor correction, and balancing of nonlinear loads," *IEEE Transactions on Power Electronics*, vol. 15, no. 3, pp. 495–507, May 2000, doi: 10.1109/63.844510.
[5] B. Singh and J. Solanki, "An implementation of an adaptive control algorithm for a three-phase shunt active filter," *IEEE Transactions on Industrial Electronics*, vol. 56, no. 8, pp. 2811–2820, Aug. 2009, doi: 10.1109/TIE.2009.2014367.
[6] H. Li, Z. Wu, and F. Liu, "A novel variable step size adaptive harmonic detecting algorithm applied to active power filter," in *Proceedings of the IEEE International Conference on Industrial Technology*, 2006, pp. 574–578. doi: 10.1109/ICIT.2006.372222.
[7] D. Suresh and S. P. Singh, "Design of single input fuzzy logic controller for shunt active power filter," *IETE Journal of Research*, vol. 61, no. 5, pp. 500–509, Sep. 2015, doi: 10.1080/03772063.2015.1024176.
[8] M. Singh and A. Chandra, "Real-time implementation of ANFIS control for renewable interfacing inverter in 3P4W distribution network," *IEEE Transactions on Industrial Electronics*, vol. 60, no. 1, pp. 121–128, 2013, doi: 10.1109/TIE.2012.2186103.
[9] B. Singh, K. Al-Haddad, and A. Chandra, "A new control approach to three-phase active filter for harmonics and reactive power compensation," *IEEE Transactions on Power Systems*, vol. 13, no. 1, pp. 133–138, 1998, doi: 10.1109/59.651624.
[10] H. Akagi, "Control strategy and site selection of a shunt active filter for damping of harmonic propagation in power distribution systems," *IEEE Transactions on Power Delivery*, vol. 12, no. 1, pp. 354–362, 1997, doi: 10.1109/61.568259.
[11] I. Moufid, Z. En-Nay, S. Naciri, H. El Moussaoui, T. Lamhamdi, and H. El Markhi, "Impact of static synchronous compensator STATCOM installation in power quality improvement," *International Journal of Power Electronics and Drive Systems (IJPEDS)*, vol. 13, no. 4, pp. 2296–2304, Dec. 2022, doi: 10.11591/ijpeds.v13.i4.pp2296-2304.
[12] J. S. Subjak and J. S. Mcquilkin, "Harmonies—causes, effects, measurements, and analysis: an update," *IEEE Transactions on Industry Applications*, vol. 26, no. 6, pp. 1034–1042, 1990, doi: 10.1109/28.62384.
[13] M. Qasim and V. Khadkikar, "Application of artificial neural networks for shunt active power filter control," *IEEE Transactions on Industrial Informatics*, vol. 10, no. 3, pp. 1765–1774, Aug. 2014, doi: 10.1109/TII.2014.2322580.
[14] B. R. Madhu, M. N. Dinesh, and B. M. Ravitheja, "Design of shunt hybrid active power filter to reduce harmonics on AC side due to non-linear loads," *International Journal of Power Electronics and Drive Systems*, vol. 9, no. 4, pp. 1926–1936, 2018, doi: 10.11591/ijpeds.v9.i4.pp1926-1936.
[15] E. Durna, "Adaptive fuzzy hysteresis band current control for reducing switching losses of hybrid active power filter," *IET Power Electronics*, vol. 11, no. 5, pp. 937–944, 2018, doi: 10.1049/iet-pel.2017.0560.
[16] S. C. Ferreira, R. B. Gonzatti, R. R. Pereira, C. H. Da Silva, L. E. B. Da Silva, and G. Lambert-Torres, "Finite control set model predictive control for dynamic reactive power compensation with hybrid active power filters," *IEEE Transactions on Industrial Electronics*, vol. 65, no. 3, pp. 2608–2617, Mar. 2018, doi: 10.1109/TIE.2017.2740819.
[17] P. Garanayak and G. Panda, "Harmonic elimination and reactive power compensation with a novel control algorithm based active power filter," *Journal of Power Electronics*, vol. 15, no. 6, pp. 1619–1627, Nov. 2015, doi: 10.6113/JPE.2015.15.6.1619.
[18] T. Rajesh and A. Nirmalkumar, "A shunt active power filter for 12 pulse converter using source current detection approach," *International Journal of Power Electronics and Drive Systems (IJPEDS)*, vol. 7, no. 1, pp. 225–234, 2016, doi: 10.11591/ijpeds.v7.i1.pp225-234.
[19] M. Mangaraj, A. K. Panda, and T. Penthia, "Investigating the performance of DSTATCOM using ADALINE based LMS algorithm," in *2016 IEEE 6th International Conference on Power Systems, ICPS 2016*, Mar. 2016, pp. 1–5. doi: 10.1109/ICPES.2016.7584062.
[20] F. Chouaf and S. Saad, "A new structure of the nine level inverter used as active power filter with a reduced number of swiches," *International Journal of Power Electronics and Drive Systems*, vol. 9, no. 1, pp. 198–209, 2018, doi: 10.11591/ijpeds.v9.i1.pp198-209.

[21] J. Ye, A. Shen, Z. Zhang, J. Xu, and F. Wu, "Systematic Design of the Hybrid Damping Method for Three-Phase Inverters with High-Order Filters," *IEEE Transactions on Power Electronics*, vol. 33, no. 6, pp. 4944–4956, 2018, doi: 10.1109/TPEL.2016.2637377.

[22] Y. Kusuma Latha, C. S. Babu, and Y. P. Obulesu, "Harmonics mitigation of industrial motor drives with active power filters in cement plant-A case study," *International Journal of Power Electronics and Drive Systems (IJPEDS)*, vol. 2, no. 1, pp. 1–8, Oct. 2012, doi: 10.11591/ijpeds.v2i1.120.

[23] J. Fei, Y. Chen, L. Liu, and Y. Fang, "Fuzzy multiple hidden layer recurrent neural control of nonlinear system using terminal sliding-mode controller," *IEEE Transactions on Cybernetics*, vol. 52, no. 9, pp. 9519–9534, Sep. 2022, doi: 10.1109/TCYB.2021.3052234.

[24] H. Akagi, E. H. Watanabe, and M. Aredes, *Instantaneous Power Theory and Applications to Power Conditioning*. Wiley-IEEE Press, 2007. doi: 10.1002/0470118938.

[25] T. Narongrit, K. Areerak, and K. Areerak, "The Comparison Study of Current Control Techniques for Active Power Filters," *World Academy of Science, Engineering and Technology 2011*, vol. 5, no. 12, pp. 471–476, 2011.

[26] S. J. Huang and J. C. Wu, "A control algorithm for three-phase three-wired active power filters under nonideal mains voltages," *IEEE Transactions on Power Electronics*, vol. 14, no. 4, pp. 753–760, Jul. 1999, doi: 10.1109/63.774215.

BIOGRAPHIES OF AUTHORS

Ramavath Chander 🆔 � [SC] ◐ is research scholar in Department of Electrical Engineering University College of Engineering (A), Osmania University, Hyderabad Telangana. He received his B.Tech., M.Tech. in Electrical Engineering from Jawaharlal Nehru Technological University Hyderabad. Telangana in 2006, 2011 respectively. His research interests include the field of digital design, power quality, industrial applications, industrial electronics, industrial informatics, power electronics, motor drives, renewable energy, FPGA applications, embedded system, artificial intelligence, intelligent control, and digital library. He can be contacted at email: chanderou19@gmail.com.

Dr. Edara Venkata Chandra Sekhara Rao 🆔 � [SC] ◐ obtained his diploma in Electrical Engineering from S.M.V.M. Polytechnic, Tanuku, West Godavari district, Andhra Pradesh. He was graduated in Electrical and Electronics Engineering from JNTU. Hyderabad. He was post-graduated with specialization in industrial drives and control from University College of Engineering, Osmania University Hyderabad Telangana. His doctorate was awarded by Osmania University in the faculty of Electrical Engineering for Design of PMH Stepper Motor using FEM and Equivalent Circuit Methods. He has 12 years of academic experience out of which 10 years in post-graduation teaching and 12 years in under graduation teaching. He has 12 years of industrial experience in electrical power generation and transmission. He has one year of research experience and guiding Eight research students. He published research paper in 12 international journals which are indexed in Scopus, 3 in international conferences (IEEE, IET and Springer) and 2 in national journals. He is Editor for two international journals and reviewer for many international journals. He reviewed papers for IEEE international conferences, held in Canada, Australia, New-Zeeland and Egypt. He is core committee member for Telangana state Energy Conservation Mission. He can be contacted at email: chandrasekhar.ev@gmail.com.

Prof. Erukula Vidyasagar 🆔 � [SC] ◐ received his B.Tech., M.Tech. and Ph.D. degrees in Electrical Engineering from Jawaharlal Nehru Technological University, Hyderabad, Telangana in 1998, 2004 and 2014, respectively. Currently, he is Professor and Head of Department in Electrical Engineering, University College of Engineering, Osmania University, Hyderabad-07. His research interests include reliability engineering and power quality. He can be contacted at email: evsuceou@gmail.com.